ACES Asian Chemical Editorial Society

DOI: 10.1002/asia.201801058

CHEMISTRY AN ASIAN JOURNAL Full Paper

Anticancer Complexes

Imine-N-Heterocyclic Carbenes as Versatile Ligands in Ruthenium(II) *p*-Cymene Anticancer Complexes: A Structure–Activity Relationship Study

Yuliang Yang, Lihua Guo,* Zhenzhen Tian, Xicheng Liu, Yuteng Gong, Hongmei Zheng, Xingxing Ge, and Zhe Liu*[a]

Abstract: A family of novel imine-N-heterocyclic carbene ruthenium(II) complexes of the general formula [(η^6-*p*-cymene)Ru(C^N)Cl]PF_6^- (where C^N is an imine-N-heterocyclic carbene chelating ligand with varying substituents) have been prepared and characterized. In this imine-N-heterocyclic carbene chelating ligand framework, there are three potential sites that can be modified, which distinguishes this class of ligand and provides a body of flexibilities and opportunities to tune the cytotoxicity of these ruthenium(II) complexes. The influence of substituent effects of three tunable domains on the anticancer activity and catalytic ability in converting coenzyme NADH to NAD^+ is investigated. This family of complexes displays an exceedingly distinct anticancer activity against A549 cancer cells, despite their close structural similarity. Complex **9** shows the highest anticancer activity in this series against A549 cancer cells (IC_{50} = 14.36 μM), with an approximately 1.5-fold better activity than the clinical platinum drug cisplatin (IC_{50} = 21.30 μM) in A549 cancer cells. Mechanistic studies reveal that complex **9** mediates cell death mainly through cell stress, including cell cycle arrest, inducing apoptosis, increasing intracellular reactive oxygen species (ROS) levels, and depolarization of the mitochondrial membrane potential (MMP). Furthermore, lysosomal damage is also detected by confocal microscopy.

Introduction

Although the research of anticancer agents has achieved remarkable progress over the past five decades, cancer remains one of the leading causes of death worldwide.[1] Given the rapid increase in cancer cases worldwide, the development of novel anticancer drugs with high performance and low toxicity has become an indispensable need. Organometallic complexes have found wide applications in various fields, particularly as catalysts[2] and anticancer agents.[3] At present, the most effective and well-studied class of metal-based anticancer agents, cisplatin and its derivatives, have been successfully applied in clinical treatment and shown high efficacy against lung, ovarian, neck, esophageal, and head cancers.[4] However, the undesirable side effects and easily acquired drug resistance of cisplatin still hinders its clinical applications and future development.[5] Therefore, obtaining new metal-based anticancer drugs, which could broaden the spectrum of treatable cancers, diminish side effects, and overcome platinum resistance, has attracted tremendous attention.[6]

Ruthenium complexes have great potential as anticancer agents as they are usually less toxic than cisplatin and hence better tolerated in vivo.[7] For example, a host of ruthenium(II) *p*-cymene complexes containing a wide range of ligands, including α-diimine ligands, imine-pyridine ligands, and pyridine-N-heterocyclic carbene (NHC) ligands, has been developed with the aim of improving their anticancer properties (Scheme 1).[8] Marchetti and co-workers developed a series of water-soluble ruthenium(II) *p*-cymene complexes containing different α-diimine ligands (**I**, Scheme 1).[8a] The cytotoxicity of these complexes strongly depended on the nature of the α-diimine *N*-substituents. Our group has designed a type of half-sandwich iridium(III) and ruthenium(II) complexes with imine-pyridyl chelating ligands and achieved good selectivity and cytotoxicity (**II**, Scheme 1).[8b,c] Overall, the metal ions and bidentate ligands around the metal mainly determined the cancer cell cytotoxicity and selectivity of these complexes. More recently, Hartinger and co-workers reported some pyridyl-NHC *p*-cymene ruthenium(II) anticancer complexes (**III**, Scheme 1)[8d] and investigated their anticancer properties and reactions with biomolecules. In this system, introduction of varying substituents gave complexes with different properties, including stability in aqueous solution, reactivity toward biomolecules, in vitro

[a] *Y. Yang, Prof. L. Guo, Z. Tian, Dr. X. Liu, Y. Gong, H. Zheng, X. Ge, Prof. Z. Liu*
Institute of Anticancer Agents Development and Theranostic Application
The Key Laboratory of Life-Organic Analysis and
Key Laboratory of Pharmaceutical Intermediates and Analysis of Natural Medicine
Department of Chemistry and Chemical Engineering, Qufu Normal University
Qufu 273165 (China)
E-mail: guolihua@qfnu.edu.cn
liuzheqd@163.com

Supporting information and the ORCID identification number(s) for the author(s) of this article can be found under: https://doi.org/10.1002/asia.201801058.

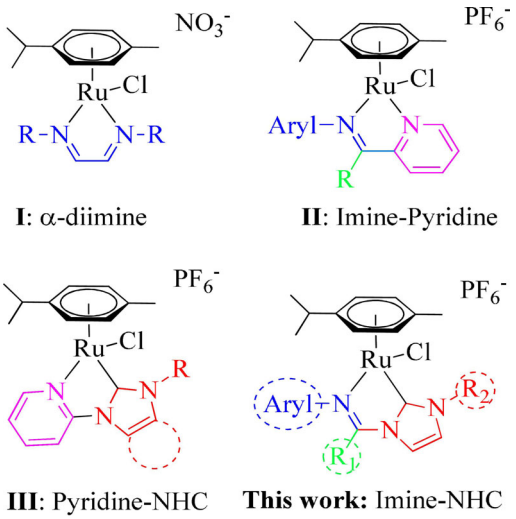

Scheme 1. The structure of relevant ruthenium(II) complexes and our current work.

cytotoxicity, and cellular uptake. These results prompted us to further investigate the effect of varying the substituents of imine-N-heterocyclic carbene chelating ligands on the chemical and biological reactivity of ruthenium(II) complexes.

Herein, a series of structurally similar half-sandwich ruthenium(II) complexes bearing versatile imine-N-heterocyclic carbene ligands has been synthesized and systematically investigated for their chemical reactivity, biological reactivity, catalytic ability in transfer hydrogenation converting coenzyme NADH into NAD^+, and in vitro cytotoxicity against A549 cancer cells. To the best of our knowledge, this form of imine-N-heterocyclic carbene half-sandwich ruthenium(II) complexes is used for the first time as anticancer agents. The effects of the substituents on anticancer activity and catalytic ability in converting coenzyme NADH to NAD^+ of the complexes were fully investigated. This family of half-sandwich ruthenium(II) complexes exhibits uncommonly different in vitro cytotoxicity, which is significantly correlated with the structure of the ligands. Initial cell death mechanistic insights, including cell cycle, apoptosis induction, mitochondrial membrane potential, reactive oxygen species (ROS) level, and lysosomal damage, are also discussed. All these studies point out that these novel ruthenium(II) organometallic complexes possess a variety of interesting biological effects that make them attractive as a potentially promising candidate for the development of anticancer agents.

Results and Discussion

Synthesis and characterization

The imine-N-heterocyclic carbene ligands (**L1**–**L10**) and novel ruthenium(II) complexes (**1**–**10**) were prepared according to well-established procedures, depicted in Scheme 2. A series of versatile imine-N-heterocyclic carbene ligands were synthesized by a coupling reaction of the corresponding imidoyl chlorides with N-substituted imidazole. Imine-N-heterocyclic carbene silver complexes were usually used as effective transfer reagents to obtain other transition-metal complexes.[9] Novel ruthenium(II) complexes **1**–**10** were synthesized in high yields (60–87%) from the corresponding (NHC)AgCl complex with $[(\eta^6\text{-}p\text{-cymene})RuCl_2]_2$ by stirring at ambient temperature overnight, and the corresponding ruthenium(II) complexes were isolated as PF_6^- salts. All the synthesized ruthenium(II) complexes were fully characterized by ^1H and ^{13}C NMR spectroscopy (Figures S1–S36 in the Supporting Information), CHN elemental analysis, and mass spectrometry (Figures S37–S54 in

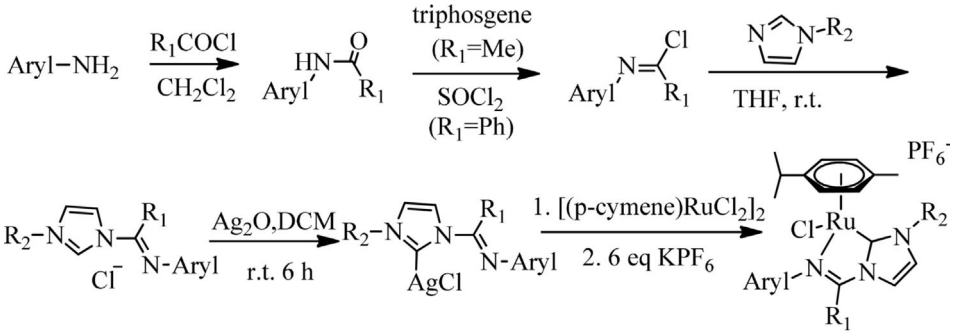

L1-L10 **1-10**

Complex	Aryl	R_1	R_2	Complex	Aryl	R_1	R_2
1	2,6-$Me_2C_6H_3$	Me	Me	**6**	2,6-$^i Pr_2C_6H_3$	Me	Me
2	2,6-$Me_2C_6H_3$	Me	Et	**7**	2,6-$^i Pr_2C_6H_3$	Me	Et
3	2,6-$Me_2C_6H_3$	Me	^{i}Pr	**8**	2,6-$^i Pr_2C_6H_3$	Me	^{i}Pr
4	2,6-$Me_2C_6H_3$	Me	^{n}Bu	**9**	2,6-$^i Pr_2C_6H_3$	Me	^{n}Bu
5	Ph	Ph	^{i}Pr	**10**	2,6-$Me_2C_6H_3$	Ph	^{i}Pr

Scheme 2. Synthetic routes for imine-N-heterocyclic carbene ligands **L1**–**L10** and $[(\eta^6\text{-}p\text{-cymene})Ru(C\text{^}N)Cl]PF_6^-$ complexes **1**–**10**.

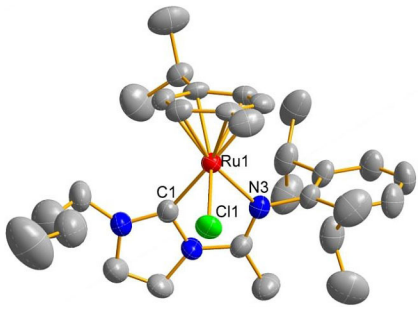

Figure 1. X-ray crystal structures of compound of [(η^6-*p*-cymene)Ru(L9)Cl]PF_6^- (**9**) with the thermal ellipsoids drawn at the 50% probability level. The hydrogen atoms and PF_6^- counterions have been omitted for clarity. Selected bond lengths (Å) and angles (deg): Ru–C (centroid) = 1.7398, Ru–C1 = 2.022(6), Ru–N3 = 2.132(5), Ru–Cl1 = 2.4026(16); C1-Ru-N3 = 76.0(2), C1-Ru-Cl1 = 78.6(2), N3-Ru-Cl1 = 87.53(14).

the Supporting Information). The characteristic peaks for the central imidazolium carbon of these complexes were at δ = 186.34–192.68 ppm in the ^{13}C NMR spectra. Additionally, the molecular structure of complex **9** was unambiguously confirmed by the X-ray crystallographic study (Figure 1 and Tables S1–S2 in the Supporting Information).

X-ray crystal structures

A single crystal suitable for X-ray diffraction analysis was obtained from the slow diffusion of petroleum ether into a nearly saturated solution of complex **9** in CH_2Cl_2/ethyl acetate. Their structures and atom numbering schemes are shown in Figure 1. Crystallographic data are shown in Table S1 (in the Supporting Information), and selected bond lengths and angles are listed in Table S2 (in the Supporting Information). As shown in Figure 1, complex **9** adopts the expected half-sandwich pseudo-octahedral three-legged piano-stool arrangement, and hence, the arene ring displays the common π-bonded η^6-coordination mode, whereas the imine-N-heterocyclic carbene-type ligand assumes a bidentate chelate coordination mode (κ^2-C,N). The two rings of the five-membered chelate ring and the imidazole ring are approximately coplanar. The Ru–Cl bond length is 2.4026(16) Å. The Ru–η^6-*p*-cymene ligand (centroid) distance is 1.7398 Å. The orthometalated Ru–C length [Ru–C = 2.022(6) Å] is shorter than Ru–N [Ru–N = 2.132(5) Å].

Stability studies

For the investigation of aqueous stability, studies were conducted by ^1H NMR spectroscopy at 310 K for complexes **1**–**10**, which were dissolved in 30% [D_6]DMSO/70% D_2O (v/v). The presence of [D_6]DMSO ensured the solubility of the complex. As shown in Figures S55–S64 (in the Supporting Information), no additional peaks were observed in the ^1H NMR spectra after 24 h. In addition, the ^{35}Cl NMR spectra for complexes **4** and **9**, recorded on solutions in 60% [D_6]DMSO/40% D_2O (v/v) after 24 h, showed no evidence of free Cl^- ions (Figures S65–S66 in the Supporting Information). It should be noted that some previously reported half-sandwich metal complexes may undergo Cl^-/H_2O exchange more easily in diluted solutions with a higher relative content of water, as in the case of cell culture.[10] As a result, complex **9** was added in water and stirred at 310 K for 24 h. Subsequently, the solid sample of complex **9** was recovered and dissolved in $CDCl_3$ to repeat the ^1H NMR spectra (Figure S67 in the Supporting Information). There was also no change in the ^1H NMR spectra, which indicated that hydrolysis also did not occur when a high content of water was employed. Complex **9** was also monitored by UV/Vis spectroscopy in 5% MeOH/95% H_2O (v/v) solution (Figure S68 in the Supporting Information) to further estimate the stability of these complexes. The results obtained by UV/Vis spectroscopy in a high content of water were consistent with the NMR analysis. Overall, the stability studies suggest that the complexes have sufficient stability for the preparation of samples for biological assays.

The structure–activity relationship study

The in vitro cytotoxicity of the ligands **L1**–**L10**, complexes **1**–**10**, and cisplatin against A549 cancer cells was examined after a 24 h exposure period by using the 3-(4,5-dimethylthiazol-2-yl)-2,5-diphenyltetrazolium bromide (MTT) assay. The widely used clinical platinum drug cisplatin was included as a control. All of the imine-N-heterocyclic carbene ligands showed very low cytotoxicity against A549 cells (> 100 μM) and they were thus deemed as inactive. On the other hand, although these ruthenium(II) complexes are structurally analogous, they had different anticancer activities. Subtle structural changes in the ligand substituents can dramatically alter the cytotoxic activities of these complexes. As depicted in Table 1 and Figure 2, complexes **1**–**4**, and **6** were inactive (> 100 μM). However, the other five complexes displayed anticancer activity toward A549 cancer cells comparable to or even higher than cisplatin. Notably, complex **9**, the most cytotoxic one against the A549 cancer cells, exhibited approximately 1.5-fold greater activity than cisplatin. Overall, the in vitro anticancer activity of the test complexes was in the following order: **9** > cisplatin > **8** > **7** > **10** > **5**.

Table 1. Inhibition of the growth of A549 cancer cells by ligands **L1**–**L10**, complexes **1**–**10**, and cisplatin.[a]

Ligand	IC_{50} [μM]	Complex	IC_{50} [μM]
L1	> 100	[(η^6-*p*-cymene)Ru(L1)Cl]PF_6 (**1**)	> 100
L2	> 100	[(η^6-*p*-cymene)Ru(L2)Cl]PF_6 (**2**)	> 100
L3	> 100	[(η^6-*p*-cymene Ru(L3)Cl]PF_6 (**3**)	> 100
L4	> 100	[(η^6-*p*-cymene)Ru(L4)Cl]PF_6 (**4**)	> 100
L5	> 100	[(η^6-*p*-cymene)Ru(L5)Cl]PF_6 (**5**)	52.16 ± 2.4
L6	> 100	[(η^6-*p*-cymene)Ru(L6)Cl]PF_6 (**6**)	> 100
L7	> 100	[(η^6-*p*-cymene)Ru(L7)Cl]PF_6 (**7**)	38.33 ± 2.3
L8	> 100	[(η^6-*p*-cymene)Ru(L8)Cl]PF_6 (**8**)	25.21 ± 1.1
L9	> 100	[(η^6-*p*-cymene)Ru(L9)Cl]PF_6 (**9**)	14.36 ± 2.4
L10	> 100	[(η^6-*p*-cymene)Ru(L10)Cl]PF_6 (**10**)	46.80 ± 3.7
		Cisplatin	21.30 ± 1.7

[a] IC_{50} values are drug concentrations necessary for 50% inhibition of cell viability. Data are presented as means ± standard deviations and cell viability is assessed after 24 h of incubation.

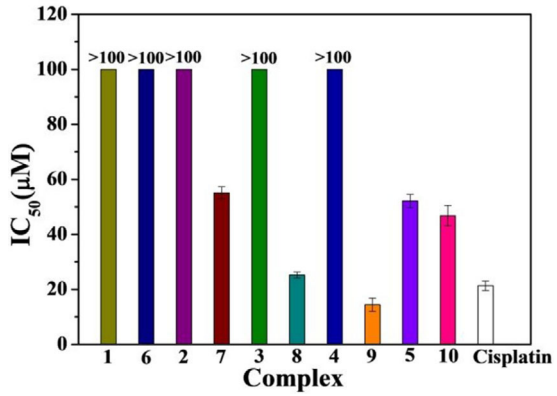

Figure 2. Inhibition of the growth of A549 cells by complexes **1**–**10** and cisplatin.

Substituent perturbations in this system can result in significant variation of anticancer activities. First, the length of the alkyl substitutions on the imidazole ring showed a significant effect on the cytotoxicity of complexes. When the tether length on the imidazole ring increased from methyl to butyl, the complexes exhibited increased cytotoxicity (complex **6**: >100 μM vs. complex **9**: 14.36 μM). The cytotoxicity followed the order of butyl > isopropyl > ethyl > methyl-substituted NHCs. It seems reasonable that, in accordance with the behavior of some previously reported potent anticancer agents,[11] the increased length of the alkyl substituents may increase the lipophilicity of these complexes and thus lead to the enhanced cytotoxicity. Next, maintaining the imidazole ring substituent unchanged and increasing the size of the *ortho* substituents on the aniline gradually, the cytotoxicity also increased and followed the order isopropyl > methyl > H-substituted aniline. For example, complexes **7**, **8**, **9**, and **10**, the IC_{50} values of which were 38.33, 25.21, 14.36, and 46.8 μM, respectively, exhibited in vitro anticancer activity significantly superior to complexes **2** (>100 μM), **3** (>100 μM), **4** (>100 μM), and **5** (52.16 μM) containing the same substituents (R^1 and R^2) against A549 cancer cell lines. Finally, the influence of the substituent at the imine carbon on anticancer activity of this class of complexes was further investigated. Replacement of the methyl group on the imine carbon by a more lipophilic phenyl ring led to enhanced anticancer efficacy (complex **3**: $IC_{50} > 100$ μM vs. complex **10**: $IC_{50} = 46.8$ μM). Pervious work has shown that the lipophilicity and cytotoxicity of the similar half-sandwich C,N and *N*,*N*-chelating iridium(III) complexes increased by the incorporation of phenyl substituents on η^5-C_5Me_5.[12] In this system, the anticancer activity of such complexes could also be tuned by regulating the lipophilicity of the substituents on the imine carbon. Overall, small structural changes on three positions of chelating ligand of these complexes can significantly alter their biological properties. These results may guide the development of the structure–activity relationships (SARs) for ruthenium-based anticancer agents and provide a rational strategy for improving their toxicological properties.

Interaction with nucleobases

The binding studies of anticancer metallodrugs with model nucleobase 9-ethylguanine (9-EtG) and 9-methyladenine (9-MeA) provided insights into their intracellular fate.[13] The reactions of complex **9** with model nucleobase 9-EtG or 9-MeA were monitored by using the ^{1}H NMR technique. Solutions of complex **9** (ca. 1 mM) and 2.0 molar equivalents of 9-EtG or 9-MeA in 50% CD_3OD/50% D_2O (v/v) were prepared, and ^{1}H NMR spectra were recorded at different time intervals at 310 K. According to the ^{1}H NMR spectra at different time intervals, no additional ^{1}H NMR peaks were observed over a period of 24 h (Figures S69–S70 in the Supporting Information). These results suggested that no reaction with model nucleobase occurred for complex **9**. Also, the formation of nucleobase adducts with these ruthenium(II) complexes were not detected by mass spectrometry. Thus, DNA may not be the major target for this type of ruthenium(II) complexes.

Reaction with NADH

Coenzyme NADH and NAD^+ play a key role in numerous biocatalyzed processes. Our previous work has reported that half-sandwich iridium(III) and ruthenium(II) anticancer complexes can oxidize NADH to generate reactive oxygen species (ROS) H_2O_2, which provides a pathway for an oxidant mechanism of action.[8b,14] To investigate the impact of this family of complexes containing three modifiable potential sites on the catalytic ability, the reactions of complexes **3**, **5**, **8**, **9**, and **10** (ca. 1 μM) with NADH (100 μM) in 5% MeOH/95% H_2O (v/v) were monitored by employing a ultraviolet/visible (UV/Vis) spectrophotometer at 298 K (Figure 3a and Figure S71 in the Supporting Information). The conversion of NADH to NAD^+ was detected by measuring the UV absorption at 339 nm by using a spectrophotometer, as NADH exhibits an absorption peak at 339 nm whereas NAD^+ does not. The turnover numbers (TONs) of complexes **3** (6.0), **5** (8.1), **8** (13.1), **9** (8.5), and **10** (7.8) were calculated by measuring the absorption difference at 339 nm (Figure 3b). The size of the *ortho* substituents on the aniline moiety, the substituent perturbations on the imine carbon, and the length of the alkyl substitutions on the imidazole ring appear to exhibit little variation on the catalytic activity of this class of complexes.

Cell cycle arrest

As most metal-based chemotherapeutic agents could disrupt the regulated cell cycle distribution, the effect of the most active complex **9** on the cell cycle perturbation in A549 cancer cells was examined by flow cytometry analysis. As shown in Figure 4, Figure S72, and Table S3 (in the Supporting Information), after treatment of A549 cells with complex **9** at 0.5, 1, and 2 equipotent concentrations of IC_{50} for 24 h, the percentage of cells at the S phase increased markedly from 22.52% to 33.25%. Meanwhile, the percentage of the cells at the G_0/G_1 phase decreased from 64.00% to 46.82%. The cells at the G_2/M phase only slightly changed. These results indicated that com-

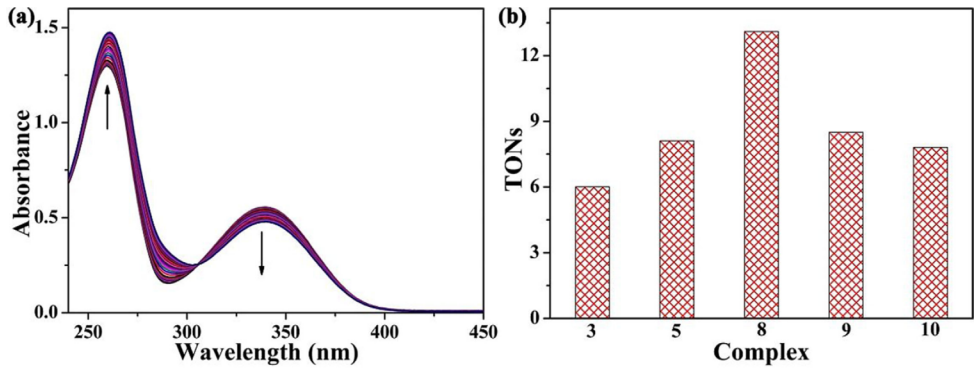

Figure 3. (a) UV/Vis spectra of the reaction of NADH (100 μM) with complex **8** (1 μM) in 5% MeOH/95% H_2O (v/v) at 298 K for 8 h. (b) The turnover numbers (TONs) of complexes **3**, **5**, **8**, **9**, and **10**.

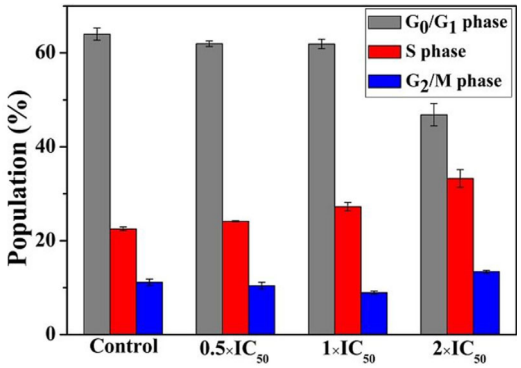

Figure 4. Flow cytometry data for cell cycle distribution of A549 cancer cells exposed to complex **9** for 24 h. Concentrations used were 0.5, 1, and 2 equipotent concentrations of IC_{50}. Cell staining for flow cytometry was carried out by using PI/RNase. Data are quoted as mean ± SD of three replicates.

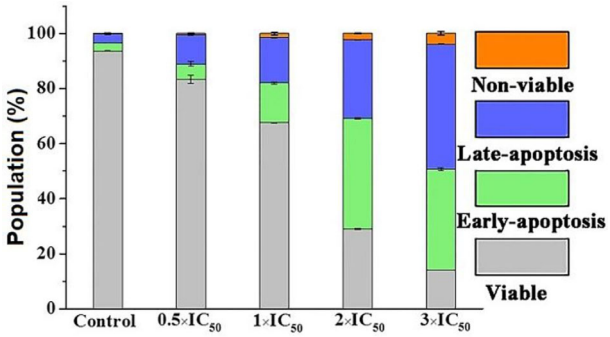

Figure 5. Apoptosis analysis of A549 cells after 24 h of exposure to complex **9** at 310 K determined by flow cytometry by using annexin V-FITC vs. PI staining. Populations for cells in four stages treated by complex **9**. Data are quoted as mean ± SD of three replicates.

plex **9** can induce perturbations of cell-cycle progression and effectively stall cells in the S phase of the cell cycle in a dose-dependent manner.

Apoptosis assay

To assess whether these ruthenium(II) complexes induce A549 cell death by apoptosis or necrosis, A549 cells were dual-stained with annexin V-FITC/propidium iodide (PI) reagents and analyzed by flow cytometry. As shown in Figure 5, Figure S73, and Table S4 (in the Supporting Information), upon incubating A549 cells with complex **9** at 0.5, 1, 2, and 3 equipotent concentrations of IC_{50} for 24 h, a dose-dependent apoptosis population was detected. At a maximum concentration ($3\times IC_{50}$), a total of 82.15% (early apoptotic + late apoptotic) of cells were undergoing enhanced apoptosis compared with the untreated group (6.21%). In addition, no strikingly increased necrotic population was detected. These results suggested that complex **9** can induce A549 cell death through a high incidence of apoptosis, and cell necrotic was not responsible for A549 cell death.

Mitochondrial membrane potential (MMP)

The change of mitochondrial membrane potential (MMP, $\Delta\psi_m$), which is a significant indicator of cell health, was detected by using 5,5′,6,6′-tetrachloro-1,1′-3,3′-tetraethyl-benzimidazolyl carbocyanine iodide (JC-1) staining and analyzed by using flow cytometry. JC-1 can be aggregated in mitochondria in a potential-dependent manner indicated by a marked red to green color shift.[15] Treatment of A549 cells with complex **9** resulted in a dose-dependent increase in the red fluorescence and decrease in green fluorescence of JC-1 (Figure 6 and Table S5 in the Supporting Information). After 24 h of treatment, the percentage of cells with mitochondrial membrane depolarization was 71.35% at a concentration of $2\times IC_{50}$, which is elevated from the vehicle-treated group (10.12%). In addition, representative JC-1 red/green ratio signals are shown in Figure S74 and Table S6 (in the Supporting Information). Treatment of A549 cells with complex **9** at concentrations of $2\times IC_{50}$ values significantly decreased the JC-1 red/green fluorescence ratios (control: 8.94 ± 1.1; $2\times IC_{50}$: 0.40 ± 0.1). This observation suggested that complex **9** can cause cancer cell death through the dysfunction of the mitochondrial membrane potential.

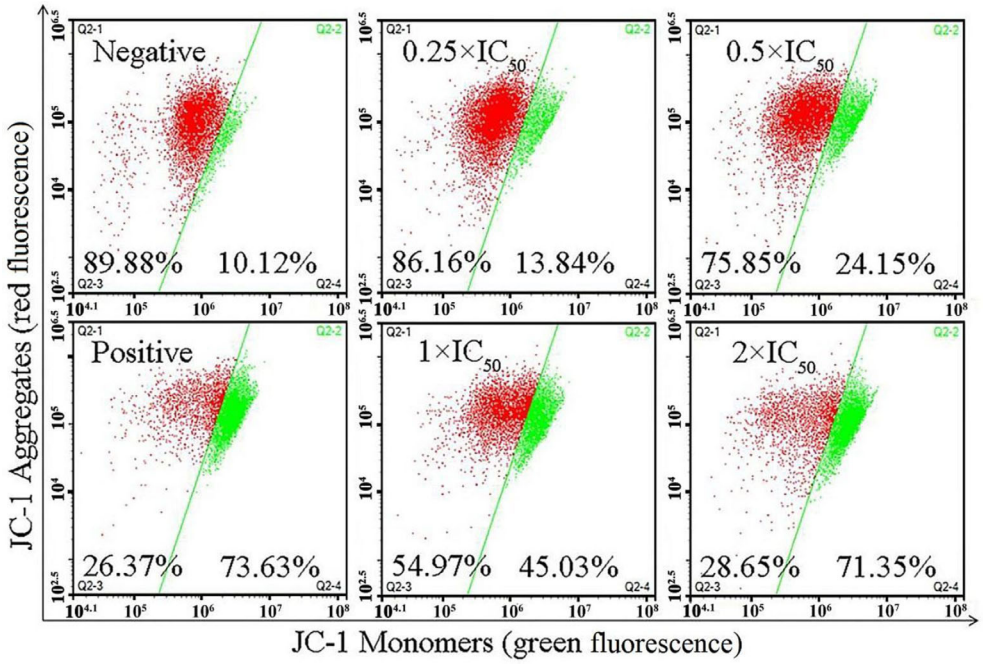

Figure 6. Changes in mitochondrial membrane potential of A549 cancer cells induced by complex **9**.

ROS determination

Perturbation of mitochondrial functions, such as the reduction of mitochondrial membrane potential (MMP), may result in over-generation of intracellular reactive oxygen species (ROS).[16] The impact of complex **9** on the number of intracellular ROS was quantified by flow cytometry with 2′,7′-dichlorodihydrofluorescein diacetate (H_2DCFDA) staining. The non-fluorescent H_2DCFDA can be converted to the highly bright 2′,7′-dichlorofluorescein (DCF) by intracellular ROS.[17] Compared with the untreated group, a dose-dependent trend in the DCF fluorescence signals was observed after a treatment period of 24 h with the test agent at concentrations of $0.25\times IC_{50}$ and $0.5\times IC_{50}$ (Figure 7 and Figure S75 in the Supporting Information), indicating that complex **9** can result in disruption of mitochondrial function through production of reactive oxygen species (ROS).

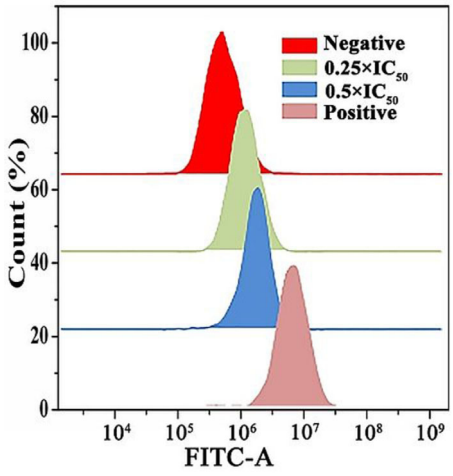

Figure 7. Analysis of ROS levels by flow cytometry after A549 cells were treated with complex **9** at 0.25 and 0.5 equipotent concentrations of IC_{50} for 24 h and stained with H_2DCFDA.

Lysosomal damage

Lysosomes play important roles in many physiological processes and cell signaling pathways. Acridine orange (AO) as an integrity indicator can be used to evaluate the dysfunction of lysosomes at the subcellular level.[18] AO is a useful probe employed to assess the lysosomal functional state at this level because it emits a concentration-dependent red/green fluorescence.[19] As shown in Figure 8, A549 cells only treated with acridine orange (5 μM) displayed distinct red fluorescence in lysosomes, indicating that the lysosomes of A549 cells under such conditions were intact. However, as the agent concentration increased, the red fluorescence of AO gradually decreased, indicating that lysosomal integrity was jeopardized by treatment with complex **9**. Thus, complex **9** can induce cell death through lysosomal damage.

Conclusion

A series of versatile half-sandwich ruthenium(II) *p*-cymene complexes, which contained different imine-N-heterocyclic carbene ligands, were explored as promising anticancer agents. The stability studies revealed that these complexes had sufficient stability for the preparation of samples for biological assays. This class of ruthenium(II) *p*-cymene complexes showed anticancer activity comparable to or even higher than cisplatin toward

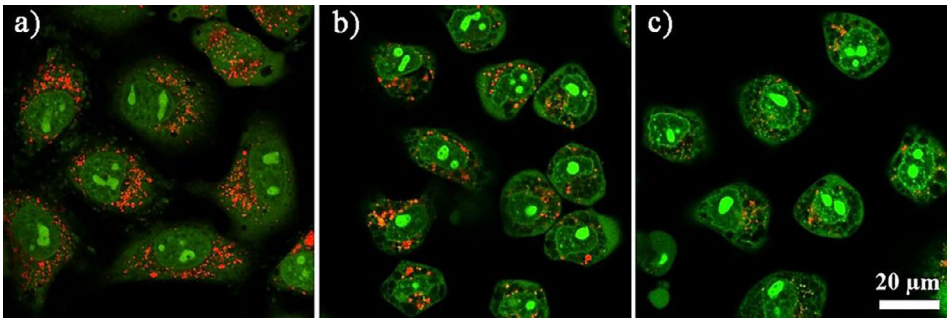

Figure 8. Observation of lysosomal disruption in A549 cells loaded with complex **9** for 6 h at 37 °C, then stained with acridine orange (5 μM) at 37 °C for 15 min. Emission was collected at 510 ± 20 nm (green) and 625 ± 20 nm (red) upon excitation at 488 nm. Scale bar: 20 μm. The cells were treated with (a) only acridine orange; (b) acridine orange and complex **9** ($1\times IC_{50}$); (c) acridine orange and complex **9** ($3\times IC_{50}$).

A549 cancer cells. The structure–activity relationship study revealed that the longer length of the alkyl substitutions on the imidazole ring, the larger size of *ortho* substituents on the aniline, and more lipophilic substituents on the imine carbon resulted in the higher anticancer activity of these ruthenium(II) complexes.

No nucleobase binding was detected for complex **9**, suggesting that DNA may not be a possible target. This type of complex gave effective catalysts for transfer hydrogenation converting coenzyme NADH into NAD^+. The effect of substituents in the three positions of the ligands on the catalytic ability seemed to be insignificant. Further mechanistic studies showed that complex **9** can trigger the arrest of cell growth at the S phase and efficiently induce early- and late-stage apoptosis in A549 cells. Simultaneously, depolarization of the mitochondrial membrane potential (MMP) and the increase in intracellular levels of the ROS were also observed. Interestingly, lysosomal damage was detected in A549 cancer cells by confocal microscopy, suggesting that these complexes may mediate cell death through lysosomal damage.

Experimental Section

General information

$RuCl_3{\cdot}nH_2O$, α-terpinene, 1-methylimidazole, 1-ethylimidazole, 1-isopropylimidazole, 1-butylimidazole, acetyl chloride, benzoyl chloride, aniline, 2,6-dimethylaniline, 2,6-diisopropylaniline, triphosgene, thionyl dichloride, silver(I) oxide, 9-ethylguanine, and 9-methyladenine were purchased from Sigma–Aldrich and used directly as such. Tetrahydrofuran was dried over sodium/benzophenone for 24 h, and dichloromethane was dried over phosphorus pentoxide for 8 h before being used. $[(\eta^6\text{-}p\text{-Cymene})RuCl_2]_2$ was prepared by using a literature procedure.[20] The intermediate products *N*-(2,6-diisopropylphenyl)acetamide, *N*-(2,6-dimethylphenyl)acetamide, *N*-phenylbenzamide, *N*-(2,6-dimethylphenyl)benzamide, *N*-(2,6-dimethylphenyl)acetimidoyl chloride, *N*-(2,6-diisopropylphenyl)acetimidoyl chloride, *N*-(2,6-dimethylphenyl)benzenecarboximidoyl chloride, and *N*-phenylbenzenecarboximidoyl chloride were prepared according to previously reported procedures.[21] The imine-N-heterocyclic carbene ligands **L1–L4**,[21a] **L5**,[21b–e] **L6–L9**,[21a] and **L10**[21b–e] were prepared according to slightly modified procedures reported previously. For the biological experiments, Dulbecco's Modified Eagle's Medium (DMEM), fetal bovine serum, penicillin/streptomycin mixture, trypsin/EDTA, phosphate-buffered saline (PBS), MTT (3-(4,5-dimethylthiazol-2-yl)-2,5-diphenyltetrazolium bromide), PI (propidium iodide), JC-1 (5,5′,6,6′-tetrachloro-1,1′,3,3′-tetraethylbenzimidazolyl carbocyanine iodide), and H_2DCFDA (2′,7′-dichlorodihydrofluorescein diacetate) were purchased from Sangon Biotech. Tested complexes were dissolved in DMSO just before the experiments, and the concentration of DMSO was 1% (v/v). ^{1}H and ^{13}C NMR spectra were recorded in 5 mm NMR tubes at ambient temperature with a Bruker Avance 500 spectrometer or a Bruker Ascend 400 spectrometer using TMS as an internal standard and $CDCl_3$ or DMSO as solvent. Mass spectra of the **L2–L5** and **L7–L10** were recorded with a Thermo LTQ Orbitrap XL (ESI^+). Mass spectra of the complexes **1–10** were recorded with an Atouflex Speed MALDI-TOF MS. Microanalysis (C, H, and N) was carried out by using a Carlo Erba model EA 1108 microanalyzer. X-ray diffraction data were collected at 298(2) K with a Bruker Smart CCD area detector with graphite-monochromated MoK_α radiation ($\lambda = 0.71073$ Å). CCDC 1848902 contains the supplementary crystallographic data for this paper. These data are provided free of charge by The Cambridge Crystallographic Data Centre.

Synthesis and characterizationsSynthesis of the ligands

General method: the imidazole with varying substituents was added dropwise to a solution of the corresponding iminochloride in dry THF (20 mL) over a period of 5 min. The mixture was stirred at ambient temperature for 20 h (**L1–L4** and **L6–L9**) or 4 days (**L5** and **L10**), and the product slowly precipitated as a white solid (**L1–L4** and **L6–L9**) or yellow solid (**L5** and **L10**). The crude product was obtained by filtration, washed with dry THF (3 × 15 mL), and dried under reduced pressure. The ^{1}H NMR spectra showed the presence of two geometric isomers (*E*/*Z*), which is similar with the compound reported previously.[21c]

[3-Methyl-1-(2,6-dimethylphenyl)iminyl-$C_3H_3N_2$]$^+$Cl$^-$ (L1): 1-Methylimidazole (0.86 g, 10.47 mmol) and *N*-(2,6-dimethylphenyl)acetimidoyl chloride (1.89 g, 10.40 mmol) were used. Yield: 82% (2.26 g, 8.57 mmol). This ligand is previously known.[21a]

[3-Ethyl-1-(2,6-dimethylphenyl)iminyl-$C_3H_3N_2$]$^+$Cl$^-$ (L2): 1-Ethylimidazole (0.69 g, 7.20 mmol) and *N*-(2,6-dimethylphenyl)acetimidoyl chloride (1.31 g, 7.21 mmol) were used. Yield: 92% (1.83 g, 6.59 mmol). ^{1}H NMR (400 MHz, $CDCl_3$), isomer 1/isomer 2 = 1:0.37 (molar ratio). Isomer 1: $\delta = 11.82$ (s, 1H, NC*H*N), 8.24 (s, 1H, imidazole-*H*), 7.49 (s, 1H, imidazole-*H*), 7.09 (m, 3H, Ar-*H*), 4.67 (q, J = 7.3 Hz, 2H, N-CH_2Me), 2.55 (s, 3H, imine-CH_3), 2.02 (s, 6H, *o*-Ar-CH_3), 1.70 ppm (t, J = 7.3 Hz, 3H, N-CH_2CH_3); isomer 2: $\delta = 9.48$ (s, 1H, NC*H*N), 7.38 (s, 1H, imidazole-*H*), 7.19 (s, 1H, imidazole-*H*), 7.04–

7.00 (m, 3H, Ar-*H*), 4.37 (q, J=7.3 Hz, 2H, N-CH_2Me), 2.28 (s, 3H, imine-CH_3), 2.24 (s, 6H, *o*-Ar-CH_3), 1.58 ppm (t, J=7.3 Hz, 3H, N-CH$_2$CH_3); ^{13}C NMR (101 MHz, $CDCl_3$): δ=173.16, 169.33, 143.19, 135.76 (NCHN), 134.65 (NCHN), 134.46, 128.56, 128.35, 127.99, 127.13, 126.14, 124.83, 122.18, 120.38, 119.94, 117.97, 45.98, 44.69, 23.08, 18.46, 17.98, 16.47, 15.64, 15.55 ppm; ESI-MS (*m/z*): calcd for $C_{15}H_{20}N_3$: 242.16572; found: 242.16255, [3-Et-1-(2,6-dimethylphenyl)iminyl-$C_3H_3N_2$]$^+$.

[3-*i*Pr-1-(2,6-dimethylphenyl)iminyl-$C_3H_3N_2$]$^+$Cl$^-$ (L3): 1-Isopropylimidazole (0.43 g, 3.90 mmol) and *N*-(2,6-dimethylphenyl)acetimidoyl chloride (0.70 g, 3.85 mmol) were used. Yield: 85% (0.96 g, 3.29 mmol). ^{1}H NMR (500 MHz, $CDCl_3$), isomer 1/isomer 2=1:0.81 (molar ratio). Isomer 1: δ=11.95 (s, 1H, NC*H*N), 8.25 (s, 1H, imidazole-*H*), 7.45 (s, 1H, imidazole-*H*), 7.08 (d, J=3.4 Hz, 2H, Ar-*H*), 7.04–6.98 (m, 1H, Ar-*H*), 5.34–5.23 (m, 1H, *i*Pr-CH_3), 2.59 (s, 3H, imine-CH_3), 2.03 (s, 6H, *o*-Ar-CH_3), 1.72 ppm (d, J=6.5 Hz, 6H, N-*i*Pr-CH_3); isomer 2: δ=9.37 (s, 1H, NC*H*N), 7.38 (s, 1H, imidazole-*H*), 7.21 (s, 1H, imidazole-*H*), 7.18–7.05 (m, 3H, Ar-*H*), 4.84–4.76 (m, 1H, *i*Pr-CH_3), 2.28 (s, 3H, imine-CH_3), 2.24 (s, 6H, *o*-Ar-CH_3), 1.61 ppm (d, J=6.5 Hz, 6H, N-*i*Pr-CH_3); ^{13}C NMR (101 MHz, $CDCl_3$): δ=173.16, 169.25, 143.24, 137.29, 135.76 (NCHN), 133.72 (NCHN), 128.57, 128.35, 128.02, 127.16, 126.18, 124.81, 120.12, 119.83, 118.46, 118.15, 54.24, 52.62, 23.18, 23.01, 18.47, 18.44, 18.00, 16.64 ppm; ESI-MS (*m/z*): calcd for $C_{16}H_{22}N_3$: 256.18137; found: 256.17816, [3-*i*Pr-1-(2,6- dimethylphenyl)iminyl-$C_3H_3N_2$]$^+$.

[3-*n*Bu-1-(2,6-dimethylphenyl)iminyl-$C_3H_3N_2$]$^+$Cl$^-$ (L4): 1-Butylimidazole (0.48 g, 3.87 mmol) and *N*-(2,6-dimethylphenyl)acetimidoyl chloride (0.70 g, 3.85 mmol) were used. Yield: 79% (0.93 g, 3.04 mmol). ^{1}H NMR (500 MHz, $CDCl_3$), isomer 1/isomer 2=1:0.52 (molar ratio). Isomer 1: δ=12.02 (s, 1H, NC*H*N), 8.23 (s, 1H, imidazole-*H*), 7.39 (s, 1H, imidazole-*H*), 7.07 (d, J=9.4 Hz, 2H, Ar-*H*), 7.05–6.97 (m, 1H, Ar-*H*), 4.59 (t, J=6.3 Hz, 2H, *n*Bu-CH_2), 2.55 (s, 3H, imine-CH_3), 2.02 (s, 6H, *o*-Ar-CH_3), 2.07–1.97 (m, 2H, *n*Bu-CH_2), 1.50–1.46 (dq, J=14.3, 7.2 Hz, 2H, *n*Bu-CH_2), 1.01 ppm (t, J=7.2 Hz, 3H, *n*Bu-CH_3); isomer 2: δ=9.38 (s, 1H, NC*H*N), 7.37 (s, 1H, imidazole-*H*), 7.18–7.12 (m, 2H, imidazole-*H* and Ar-*H*), 7.04–7.01 (d, J=9.4 Hz, 2H, Ar-*H*), 4.29 (t, J=6.3 Hz, 2H, *n*Bu-CH_2), 2.28 (s, 3H, imine-CH_3), 2.24 (s, 6H, *o*-Ar-CH_3), 1.89–1.86 (m, 2H, *n*Bu-CH_2), 1.41–1.33 (dq, J=14.3, 7.2 Hz, 2H, *n*Bu-CH_2), 0.97 ppm (t, J=7.2 Hz, 3H, *n*Bu-CH_3); ^{13}C NMR (101 MHz, $CDCl_3$): δ=173.13, 169.35, 143.18, 135.78 (NCHN), 134.92 (NCHN), 134.53, 128.56, 128.36, 127.98, 127.08, 126.14, 124.84, 122.44, 120.67, 119.87, 117.88, 50.46, 49.34, 32.20, 32.06, 23.08, 19.53, 19.39, 18.48, 18.00, 16.53, 13.48, 13.38 ppm; ESI-MS (*m/z*): calcd for $C_{17}H_{24}N_3$: 270.19702; found: 270.19351, [3-*n*Bu-1-(2,6-dimethylphenyl)iminyl-$C_3H_3N_2$]$^+$.

[3-*i*Pr-1-{C(C_6H_5)N(C_6H_5)}$C_3H_3N_2$]$^+$Cl$^-$ (L5): 1-Isopropylimidazole (1.14 g, 10.35 mmol) and *N*-phenylbenzenecarboximidoyl chloride (2.23 g, 10.34 mmol) were used. Yield: 85% (2.88 g, 8.84 mmol). ^{1}H NMR (500 MHz, $CDCl_3$), isomer 1/isomer 2=1:0.78 (molar ratio). Isomer 1: δ=9.14 (s, 1H, NC*H*N), 7.89 (m, 2H, imidazole-*H*), 7.44 (m, 1H, Ar-*H*), 7.40 (m, 1H, Ar-*H*), 7.30 (t, J=7.6 Hz, 2H, Ar-*H*), 7.21–7.19 (d, J=2.7 Hz, 3H, Ar-*H*), 6.93 (d, J=2.7 Hz, 3H, Ar-*H*), 4.79–4.68 (m, 1H, *i*Pr-CH_3), 1.62 ppm (d, J=6.6 Hz, 6H, *N*-*i*Pr-CH_3); isomer 2: δ=12.91 (s, 1H, NC*H*N), 7.67 (d, J=6.0 Hz, 2H, imidazole-*H*), 7.58–7.52 (m, 1H, Ar-*H*), 7.51–7.48 (m, 2H, Ar-*H*), 7.39–7.36 (m, 2H, Ar-*H*), 7.19–7.14 (m, 5H, Ar-*H*), 3.80–3.68 (m, 1H, *i*Pr-CH_3), 1.73 ppm (d, J=6.6 Hz, 6H, *N*-*i*Pr-CH_3); ^{13}C NMR (101 MHz, $CDCl_3$): δ=171.05, 165.90, 138.18, 134.92 (NCHN), 133.85 (NCHN), 132.06, 131.78, 129.83, 129.52, 129.27, 129.04, 128.99, 128.70, 127.40, 127.28, 125.62, 124.95, 124.44, 121.37, 120.49, 120.17, 118.22, 54.19, 52.64, 23.18, 22.88 ppm; ESI-MS(*m/z*): calcd for $C_{19}H_{20}N_3$: 290.16572; found: 290.16464, [3-*i*Pr-1-{C(C_6H_5)N(C_6H_5)}$C_3H_3N_2$]$^+$.

[3-Me-1-(2,6-diisopropylphenyl)iminyl-$C_3H_3N_2$]$^+$Cl$^-$ (L6): 1-Methylimidazole (0.28 g, 3.41 mmol) and *N*-(2,6-diisopropylphenyl)acetimidoyl chloride (0.79 g, 3.32 mmol) were used. Yield: 61% (0.65 g, 2.03 mmol). This ligand is previously known.[21a]

[3-Et-1-(2,6-diisopropylphenyl)iminyl-$C_3H_3N_2$]$^+$Cl$^-$ (L7): 1-Ethylimidazole (0.32 g, 3.33 mmol) and *N*-(2,6-diisopropylphenyl)acetimidoyl chloride (0.80 g, 3.36 mmol) were used. Yield: 68% (0.75 g, 2.25 mmol). ^{1}H NMR (500 MHz, $CDCl_3$), isomer 1/isomer 2=1:0.68 (molar ratio). Isomer 1: δ=11.97 (s, 1H, NC*H*N), 8.22 (s, 1H, imidazole-*H*), 7.57 (s, 1H, imidazole-*H*), 7.18 (s, 3H, Ar-*H*), 4.69 (q, J=6.6 Hz, 2H, *N*-CH_2Me), 2.68–2.59 (m, 2H, *i*Pr-C*H*), 2.56 (s, 3H, imine-CH_3), 1.71 (t, J=6.6 Hz, 3H, *N*-CH$_2$CH_3), 1.17 (d, J=6.8 Hz, 6H, *i*Pr-CH_3), 1.12 ppm (d, J=6.1 Hz, 6H, *i*Pr-CH_3); isomer 2: δ=9.55 (s, 1H, NC*H*N), 7.36 (s, 1H, imidazole-*H*), 7.23 (s, 1H, imidazole-*H*), 7.21–7.16 (m, 3H, Ar-*H*), 4.40 (q, J=6.6 Hz, 2H, *N*-CH_2Me), 3.22–3.08 (m, 2H, *i*Pr-C*H*), 2.26 (s, 3H, imine-CH_3), 1.59 (t, J=6.6 Hz, 3H, *N*-CH$_2$CH_3), 1.25–1.19 ppm (dd, J=6.8 Hz, 7.8 Hz, 12H, *i*Pr-CH_3); ^{13}C NMR (101 MHz, $CDCl_3$): δ=173.59, 170.05, 146.85, 146.49, 136.50 (NCHN), 134.87 (NCHN), 129.08, 128.32, 125.50, 123.92, 123.53, 123.41, 122.08, 120.21, 119.95, 117.78, 44.75, 28.75, 28.50, 24.41, 23.67, 23.21, 22.84, 15.72 ppm; ESI-MS (*m/z*): calcd for $C_{19}H_{28}N_3$: 298.22832; found: 298.22723, [3-Et-1-(2,6-diisopropylphenyl)iminyl-$C_3H_3N_2$]$^+$.

[3-*i*Pr-1-(2,6-diisopropylphenyl)iminyl-$C_3H_3N_2$]$^+$Cl$^-$ (L8): 1-Isopropylimidazole (0.39 g, 3.54 mmol) and *N*-(2,6-diisopropylphenyl)acetimidoyl chloride (0.83 g, 3.49 mmol) were used. Yield: 63% (0.77 g, 2.21 mmol). ^{1}H NMR (500 MHz, $CDCl_3$), isomer 1/isomer 2=1:0.2 (molar ratio). Isomer 1: δ=12.08 (s, 1H, NC*H*N), 8.23 (s, 1H, imidazole-*H*), 7.51 (s, 1H, imidazole-*H*), 7.18 (s, 3H, Ar-*H*), 5.41–5.29 (m, 1H, *i*Pr-C*H*), 2.67–2.61 (m, 2H, *i*Pr-C*H*), 2.61 (s, 3H, imine-CH_3), 1.73 (d, J=6.6 Hz, 6H, *i*Pr-CH_3), 1.17 (d, J=6.8 Hz, 6H, *i*Pr-CH_3), 1.12 ppm (d, J=6.8 Hz, 6H, *i*Pr-CH_3); isomer 2: δ=9.29 (s, 1H, NC*H*N), 7.40 (s, 1H, imidazole-*H*), 7.24 (s, 1H, imidazole-*H*), 7.21–7.10 (s, 3H, Ar-*H*), 4.83–4.75 (m, 1H, *i*Pr-C*H*), 3.22–3.07 (m, 2H, *i*Pr-C*H*), 2.26 (s, 3H, imine-CH_3), 1.61 (d, J=6.6 Hz, 6H, *i*Pr-CH_3), 1.25–1.19 ppm (dd, J=6.8 Hz, 7.6 Hz, 12H, *i*Pr-CH_3); ^{13}C NMR (101 MHz, $CDCl_3$): δ=173.60, 170.15, 140.70, 137.51 (NCHN), 136.50 (NCHN), 133.69, 128.26, 125.46, 123.92, 123.50, 123.36, 120.10, 119.96, 118.47, 117.94, 54.25, 52.63, 28.72, 28.46, 24.41, 23.68, 23.21, 23.07, 22.82, 17.06 ppm; ESI-MS (*m/z*): calcd for $C_{20}H_{30}N_3$: 312.24397; found: 312.24039, [3-*i*Pr-1-(2,6-diisopropylphenyl)iminyl-$C_3H_3N_2$]$^+$.

[3-*n*Bu-1-(2,6-diisopropylphenyl)iminyl-$C_3H_3N_2$]$^+$Cl$^-$ (L9): 1-Butylimidazole (0.42 g, 3.38 mmol) and *N*-(2,6-diisopropylphenyl)acetimidoyl chloride (0.80 g, 3.36 mmol) was used. Yield: 49% (0.60 g, 1.66 mmol). ^{1}H NMR (500 MHz, $CDCl_3$), isomer 1/isomer 2=1:1.35 (molar ratio). Isomer 1: δ=12.00 (s, 1H, NC*H*N), 8.21 (s, 1H, imidazole-*H*), 7.50 (s, 1H, imidazole-*H*), 7.19–7.17 (s, 3H, Ar-*H*), 4.61 (t, J=7.2 Hz, 2H, *n*Bu-CH_2), 2.68–2.58 (m, 2H, *i*Pr-C*H*), 2.56 (s, 3H, imine-CH_3), 2.08–1.98 (m, 2H, *n*Bu-CH_2), 1.48 (dq, J=15.0, 7.5 Hz, 2H, *n*Bu-CH_2), 1.16 (d, J=6.6 Hz, 6H, *i*Pr-CH_3), 1.11 (d, J=6.6 Hz, 6H, *i*Pr-CH_3), 1.03–0.99 ppm (t, J=7.4 Hz, 3H, *n*Bu-CH_3); isomer 2: δ=9.48 (s, 1H, NC*H*N), 7.46–7.32 (s, 1H, imidazole-*H*), 7.29 (s, 1H, imidazole-*H*), 7.28–7.20 (s, 3H, Ar-*H*), 4.32 (t, J=7.2 Hz, 2H, *n*Bu-CH_2), 3.21–3.08 (m, 2H, *i*Pr-C*H*), 2.26 (s, 3H, imine-CH_3), 1.93–1.85 (m, 2H, *n*Bu-CH_2), 1.40–1.32 (dq, J=15.0, 7.5 Hz, 2H, *n*Bu-CH_2), 1.26–1.18 (m, 12H, *i*Pr-CH_3), 0.97 ppm (t, J=7.4 Hz, 3H, *n*Bu-CH_3); ^{13}C NMR (101 MHz, $CDCl_3$): δ=169.98, 146.86, 146.48, 136.51 (NCHN), 135.15 (NCHN), 131.48, 129.08, 128.33, 125.51, 123.93, 123.53, 123.42, 120.47, 119.96, 117.68, 50.57, 49.40, 32.24, 28.76, 28.50, 24.42, 23.67, 23.24, 22.74, 19.60, 19.42, 17.02, 13.40 ppm; ESI-MS(*m/z*): calcd for $C_{21}H_{32}N_3$: 326.25962; found: 326.25842, [3-*n*Bu-1-(2,6-diisopropylphenyl)iminyl-$C_3H_3N_2$]$^+$.

[3-*i*Pr-1-{C(C_6H_5)N(2,6-$Me_2C_6H_3$)}$C_3H_3N_2$]$^+Cl^-$ (L10): 1-Isopropylimidazole (1.05 g, 9.53 mmol) and *N*-(2,6-dimethylphenyl)benzenecarboximidoyl chloride (2.12 g, 8.70 mmol) were used. Yield: 72% (2.23 g, 6.30 mmol). ^{1}H NMR (500 MHz, $CDCl_3$), isomer 1/isomer 2 = 1:0.66 (molar ratio). Isomer 1: δ = 10.46 (s, 1H, NC*H*N), 7.94 (s, 2H, imidazole-*H*), 7.50–7.47 (m, 1H, Ar-*H*), 7.40 (q, *J* = 8.0 Hz, 4H, Ar-*H*), 6.91 (dt, *J* = 8.9, 5.7 Hz, 3H, Ar-*H*), 5.54 (m, 1H, *i*Pr-C*H*), 2.05 (s, 6H, *o*-Ar-CH_3), 1.69 ppm (d, *J* = 6.6 Hz, 6H, *i*Pr-CH_3); isomer 2: δ = 9.41 (s, 1H, NC*H*N), 8.00 (d, *J* = 7.3 Hz, 2H, imidazole-*H*), 7.98–7.96 (m, 1H, Ar-*H*), 7.76 (d, *J* = 6.0 Hz, 2H, Ar-*H*), 7.58–7.47 (m, 2H, Ar-*H*), 7.35 (s, 2H, Ar-*H*), 7.29 (s, 1H, Ar-*H*), 4.95–4.87 (m, 1H, *i*Pr-C*H*), 2.30 (s, 6H, *o*-Ar-CH_3), 1.58 ppm (d, *J* = 6.6 Hz, 6H, *i*Pr-CH_3); ^{13}C NMR (101 MHz, $CDCl_3$): δ = 172.50, 166.07, 148.18, 143.25, 136.31 (NCHN), 135.80 (NCHN), 134.40, 134.24, 133.77, 132.43, 131.72, 129.36, 128.83, 128.66, 128.17, 127.44, 127.28, 126.39, 124.72, 120.70, 120.12, 118.31, 54.14, 52.52, 23.20, 22.88, 18.51, 18.47 ppm; ESI-MS(*m/z*): calcd for $C_{21}H_{24}N_3$: 318.19702; found: 318.19586, [3-*i*Pr-1-{C(C_6H_5)N(2,6-$Me_2C_6H_3$)}$C_3H_3N_2$]$^+$.

Synthesis of the complexes

General method: The imidazolium salt **L** (0.10 mmol) was dissolved in dry dichloromethane (15.0 mL) and the solution was added to a round-bottomed flask containing a stirrer. Ag_2O (0.12 mmol) was then added and the reaction mixture stirred in the absence of light for 6 h. The mixture was filtered through Celite to remove excess Ag_2O. The filtrate was transferred to another round-bottomed flask, which was charged with [(η^6-*p*-cymene)RuCl_2]$_2$ (0.05 mmol) and the mixture was stirred at ambient temperature overnight. KPF_6 (0.60 mmol) was added with stirring and further stirred for 30 min at ambient temperature. The crude product was filtered and the solvent was removed under reduced pressure. The resulting solid was recrystallized by diffusion at room temperature.

[(η^6-*p*-Cymene)Ru(L1)Cl]PF_6 (1): Yield: 42.4 mg (66%). ^{1}H NMR (500 MHz, $CDCl_3$): δ = 7.54 (s, 1H, imidazole-*H*), 7.29 (d, *J* = 5.2 Hz, 1H, imidazole-*H*), 7.24 (dd, *J* = 8.7, 4.0 Hz, 3H, Ar-*H*), 5.67 (d, *J* = 5.4 Hz, 1H, *p*-cymene-*H*), 5.33 (d, *J* = 6.1 Hz, 1H, *p*-cymene-*H*), 4.98 (d, *J* = 6.2 Hz, 1H, *p*-cymene-*H*), 4.87 (d, *J* = 6.1 Hz, 1H, *p*-cymene-*H*), 4.15 (s, 3H, N-CH_3), 2.63–2.54 (m, 1H, *p*-cymene-C*H*-*i*Pr_2), 2.38 (s, 3H, *o*-aniline-CH_3), 2.34 (s, 3H, *o*-aniline-CH_3), 2.24 (s, 3H, imine-CH_3), 2.07 (s, 3H, *p*-cymene-CH_3), 1.18 (d, *J* = 7.0 Hz, 3H, *p*-cymene-CH_3-*i*Pr), 1.14 ppm (d, *J* = 6.8 Hz, 3H, *p*-cymene-CH_3-*i*Pr); ^{13}C NMR (101 MHz, $CDCl_3$): δ = 189.03 (NHC carbon-Ru), 163.73, 146.76, 132.40, 129.93, 129.13, 128.99, 128.20, 126.11, 118.07, 112.24, 106.90, 91.20, 86.85, 85.27, 84.98, 38.61, 31.57, 23.88, 21.65, 20.06, 19.23, 17.94, 14.97 ppm; ESI-MS (*m/z*): calcd for $C_{24}H_{31}ClN_3Ru$: 498.046; found: 497.903, [(η^6-*p*-cymene)Ru(L1)Cl]$^+$; elemental analysis calcd (%) for $C_{24}H_{31}N_3ClRuPF_6$: C 44.83, H 4.86, N 6.53; found: C 44.99, H 4.71, N 6.69.

[(η^6-*p*-Cymene)Ru(L2)Cl]PF_6 (2): Yield: 38.1 mg (58%). ^{1}H NMR (500 MHz, $CDCl_3$): δ = 7.60 (d, *J* = 2.3 Hz, 1H, imidazole-*H*), 7.33 (d, *J* = 2.3 Hz, 1H, imidazole-*H*), 7.29–7.26 (m, 1H, Ar-*H*), 7.25–7.22 (m, 2H, Ar-*H*), 5.66 (d, *J* = 6.2 Hz, 1H, *p*-cymene-*H*), 5.31 (d, *J* = 6.1 Hz, 1H, *p*-cymene-*H*), 4.98 (d, *J* = 6.2 Hz, 1H, *p*-cymene-*H*), 4.88 (d, *J* = 6.1 Hz, 1H, *p*-cymene-*H*), 4.51 (q, *J* = 7.4 Hz, 2H, N-CH_2Me), 2.65–2.54 (m, 1H, *p*-cymene-C*H*-*i*Pr_2), 2.38 (s, 3H, *o*-aniline-CH_3), 2.34 (s, 3H, *o*-aniline-CH_3), 2.22 (s, 3H, imine-CH_3), 2.05 (s, 3H, *p*-cymene-CH_3), 1.64 (t, *J* = 7.3 Hz, 3H, N-CH_2CH_3), 1.16 (d, *J* = 7.0 Hz, 3H, *p*-cymene-CH_3-*i*Pr), 1.13 ppm (d, *J* = 6.8 Hz, 3H, *p*-cymene-CH_3-*i*Pr); ^{13}C NMR (101 MHz, $CDCl_3$): δ = 188.00 (NHC carbon-Ru), 163.62, 146.78, 132.41, 129.94, 129.17, 129.00, 128.22, 123.45, 118.58, 112.66, 106.25, 91.03, 87.06, 85.14, 85.10, 46.88, 31.51, 23.79, 21.71, 20.11, 19.18, 17.95, 15.46, 15.01 ppm; ESI-MS (*m/z*): calcd for $C_{25}H_{33}ClN_3Ru$: 512.141; found: 511.907, [(η^6-*p*-cymene)Ru(L2)Cl]$^+$; elemental analysis calcd (%) for $C_{25}H_{33}N_3ClRuPF_6$: C 45.70, H 5.06, N 6.40; found: C 45.86, H 5.11, N 6.39.

[(η^6-*p*-cymene)Ru(L3)Cl]PF_6 (3): Yield: 58.4 mg (87%). ^{1}H NMR (500 MHz, $CDCl_3$): δ = 7.62 (d, *J* = 2.3 Hz, 1H, imidazole-*H*), 7.31 (d, *J* = 2.3 Hz, 1H, imidazole-*H*), 7.24 (dd, *J* = 8.6, 4.5 Hz, 3H, Ar-*H*), 5.58 (d, *J* = 6.2 Hz, 1H, *p*-cymene-*H*), 5.30 (d, *J* = 6.0 Hz, 1H, *p*-cymene-*H*), 5.04–4.93 (m, 2H, *p*-cymene-*H* and N-C*H*-*i*Pr_2), 4.91 (d, *J* = 6.0 Hz, 1H, *p*-cymene-*H*), 2.64–2.56 (m, 1H, *p*-cymene-C*H*-*i*Pr_2), 2.38 (s, 3H, *o*-aniline-CH_3), 2.33 (s, 3H, *o*-aniline-CH_3), 2.22 (s, 3H, imine-CH_3), 2.08 (s, 3H, *p*-cymene-CH_3), 1.79 (d, *J* = 6.8 Hz, 3H, *N*-CH_3-*i*Pr), 1.56 (d, *J* = 6.6 Hz, 3H, *N*-CH_3-*i*Pr), 1.18 (d, *J* = 7.0 Hz, 3H, *p*-cymene-CH_3-*i*Pr), 1.14 ppm (d, *J* = 6.8 Hz, 3H, *p*-cymene-CH_3-*i*Pr); ^{13}C NMR (101 MHz, $CDCl_3$): δ = 186.85 (NHC carbon-Ru), 163.63, 146.78, 132.45, 129.93, 129.30, 129.00, 128.23, 120.25, 119.21, 112.95, 90.49, 87.24, 85.43, 84.80, 54.39, 31.45, 23.82, 23.67, 22.96, 21.81, 20.12, 19.28, 17.97, 15.02 ppm; ESI-MS (*m/z*): calcd for $C_{26}H_{35}ClN_3Ru$: 526.156; found: 526.1267, [(η^6-*p*-cymene)Ru(L3)Cl]$^+$; elemental analysis calcd (%) for $C_{26}H_{35}N_3ClRuPF_6$: C 46.53, H 5.26, N 6.26; found: C 46.39, H 5.31, N 6.50.

[(η^6-*p*-cymene)Ru(L4)Cl]PF_6 (4): Yield: 50.0 mg (73%). ^{1}H NMR (400 MHz, $CDCl_3$): δ = 7.56 (s, 1H, imidazole-*H*), 7.25 (s, 4H, imidazole-*H* and Ar-*H*), 5.50 (d, *J* = 5.9 Hz, 1H, *p*-cymene-*H*), 5.33 (d, *J* = 5.5 Hz, 1H, *p*-cymene-*H*), 4.91 (dd, *J* = 10.8, 6.4 Hz, 2H, *p*-cymene-*H*), 4.50–4.37 (m, 2H, *n*Bu-CH_2), 2.68–2.59 (m, 1H, *p*-cymene-C*H*-*i*Pr_2), 2.39 (s, 3H, *o*-aniline-CH_3), 2.34 (s, 3H, *o*-aniline-CH_3), 2.24 (s, 3H, imine-CH_3), 2.09 (s, 3H, *p*-cymene-CH_3), 2.04–1.98 (m, 2H, *n*Bu-CH_2), 1.53–1.46 (m, 2H, *n*Bu-CH_2), 1.18 (d, *J* = 6.9 Hz, 3H, *p*-cymene-CH_3-*i*Pr), 1.14 (d, *J* = 6.8 Hz, 3H, *p*-cymene-CH_3-*i*Pr), 1.04 ppm (t, *J* = 7.5 Hz, 3H, *n*Bu-CH_3); ^{13}C NMR (101 MHz, $CDCl_3$): δ = 187.86 (NHC carbon-Ru), 163.68, 146.79, 132.39, 129.91, 129.31, 129.02, 128.23, 123.96, 118.42, 113.24, 105.62, 90.79, 87.20, 85.18, 84.95, 51.59, 31.79, 31.46, 23.76, 21.59, 20.14, 19.98, 19.18, 17.99, 15.01, 13.77 ppm; ESI-MS (*m/z*): calcd for $C_{27}H_{37}ClN_3Ru$: 540.172; found: 539.978, [(η^6-*p*-cymene)Ru(L4)Cl]$^+$; elemental analysis calcd (%) for $C_{27}H_{37}N_3ClRuPF_6$: C 47.34, H 5.44, N 6.13; found: C 47.56, H 5.31, N 6.19.

[(η^6-*p*-Cymene)Ru(L5)Cl]PF_6 (5): Yield: 39.5 mg (56%). ^{1}H NMR (500 MHz, DMSO): δ = 7.99 (d, *J* = 2.4 Hz, 1H, imidazole-*H*), 7.52 (dd, *J* = 13.7, 4.8 Hz, 4H, imidazole-*H* and Ar-*H*), 7.39 (s, 4H, Ar-*H*), 7.29 (t, *J* = 8.3 Hz, 3H, Ar-*H*), 6.01 (d, *J* = 6.1 Hz, 1H, *p*-cymene-*H*), 5.52 (d, *J* = 6.1 Hz, 1H, *p*-cymene-*H*), 5.47 (d, *J* = 6.2 Hz, 1H, *p*-cymene-*H*), 5.42 (d, *J* = 6.1 Hz, 1H, *p*-cymene-*H*), 5.08–4.99 (m, 1H, N-C*H*-*i*Pr_2), 2.57–2.52 (m, 1H, *p*-cymene-C*H*-*i*Pr_2), 2.11 (s, 3H, *p*-cymene-CH_3), 1.75 (d, *J* = 6.7 Hz, 3H, N-CH_3-*i*Pr), 1.45 (d, *J* = 6.6 Hz, 3H, N-CH_3-*i*Pr), 1.04 (d, *J* = 6.9 Hz, 3H, *p*-cymene-CH_3-*i*Pr), 1.02 ppm (d, *J* = 6.9 Hz, 3H, *p*-cymene-CH_3-*i*Pr); ^{13}C NMR (101 MHz, DMSO): δ = 188.86 (NHC carbon-Ru), 162.47, 150.11, 132.46, 129.75, 129.65, 129.60, 128.10, 125.81, 123.83, 123.69, 121.76, 120.83, 107.57, 92.39, 89.07, 88.19, 85.00, 54.32, 31.37, 23.73, 22.93, 22.70, 22.55, 19.14 ppm; ESI-MS (*m/z*): calcd for $C_{29}H_{33}ClN_3Ru$: 560.141; found: 559.984, [(η^6-*p*-cymene)Ru(L5)Cl]$^+$; elemental analysis calcd (%) for $C_{29}H_{33}N_3ClRuPF_6$: C 49.40, H 4.72, N 5.96; found: C 48.99, H 4.81, N 5.73.

[(η^6-*p*-Cymene)Ru(L6)Cl]PF_6 (6): Yield: 56.6 mg (81%). ^{1}H NMR (500 MHz, $CDCl_3$): δ = 7.54 (d, *J* = 1.9 Hz, 1H, imidazole-*H*), 7.44 (t, *J* = 7.7 Hz, 1H, imidazole-*H*), 7.39–7.35 (m, 1H, Ar-*H*), 7.35–7.30 (m, 2H, Ar-*H*), 5.97 (d, *J* = 6.3 Hz, 1H, *p*-cymene-*H*), 5.21 (d, *J* = 6.0 Hz, 1H, *p*-cymene-*H*), 5.05 (d, *J* = 6.2 Hz, 1H, *p*-cymene-*H*), 5.02 (d, *J* = 6.1 Hz, 1H, *p*-cymene-*H*), 4.16 (s, 3H, N-CH_3), 3.54–3.45 (m, 1H, *o*-aniline-C*H*-*i*Pr_2), 2.55–2.43 (m, 2H, *o*-aniline-C*H*-*i*Pr_2 and *p*-cymene-C*H*-*i*Pr_2), 2.42 (s, 3H, *p*-cymene-CH_3), 2.25 (s, 3H, imine-CH_3), 1.45 (d,

J=6.7 Hz, 3H, *o*-aniline-CH_3-*i*Pr$_2$), 1.26 (d, J=6.6 Hz, 3H, *o*-aniline-CH_3-*i*Pr$_2$), 1.17 (d, J=7.0 Hz, 3H, *p*-cymene-CH_3-*i*Pr), 1.15 (d, J=6.6 Hz, 3H, *o*-aniline-CH_3-*i*Pr$_2$), 1.13 (d, J=6.9 Hz, 3H, *p*-cymene-CH_3-*i*Pr), 0.95 ppm (d, J=6.8 Hz, 3H, *o*-aniline-CH_3-*i*Pr$_2$); ^{13}C NMR (101 MHz, $CDCl_3$): δ=188.57 (NHC carbon-Ru), 164.16, 143.86, 143.06, 140.25, 129.07, 126.37, 125.78, 124.81, 118.19, 111.27, 109.07, 90.40, 86.46, 85.96, 82.64, 38.72, 31.04, 27.84, 27.69, 25.75, 25.07, 23.99, 23.83, 22.16, 19.14, 17.29 ppm; ESI-MS (*m/z*): calcd for $C_{28}H_{39}ClN_3Ru$: 554.188; found: 554.019, [(η^6-*p*-cymene)Ru(L6)Cl]$^+$; elemental analysis calcd (%) for $C_{28}H_{39}N_3ClRuPF_6$: C 48.10, H 5.62, N 6.01; found: C 48.32, H 5.51, N 6.09.

[(η^6-*p*-Cymene)Ru(L7)Cl]PF$_6$ (7): Yield: 53.5 mg (75%). ^{1}H NMR (500 MHz, $CDCl_3$): δ=7.60 (s, 1H, imidazole-*H*), 7.43 (t, J=7.7 Hz, 1H, imidazole-*H*), 7.36 (d, J=6.9 Hz, 2H, Ar-*H*), 7.34 (d, J=7.7 Hz, 1H, Ar-*H*), 5.95 (d, J=6.3 Hz, 1H, *p*-cymene-*H*), 5.20 (d, J=6.0 Hz, 1H, *p*-cymene-*H*), 5.04 (t, J=5.6 Hz, 2H, *p*-cymene-*H*), 4.60–4.47 (q, J=7.2 Hz, 2H, N-CH_2Me), 3.55–3.45 (m, 1H, *o*-aniline-C*H*-*i*Pr$_2$), 2.56–2.43 (m, 2H, *o*-aniline-C*H*-*i*Pr$_2$ and *p*-cymene-C*H*-*i*Pr$_2$), 2.42 (s, 3H, *p*-cymene-CH_3), 2.24 (s, 3H, imine-CH_3), 1.64 (t, J=7.3 Hz, 3H, N-CH$_2$CH_3), 1.45 (d, J=6.7 Hz, 3H, *o*-aniline-CH_3-*i*Pr$_2$), 1.25 (d, J=6.6 Hz, 3H, *o*-aniline-CH_3-*i*Pr$_2$), 1.16 (d, J=7.0 Hz, 3H, *p*-cymene-CH_3-*i*Pr), 1.14 (d, J=6.6 Hz, 3H, *o*-aniline-CH_3-*i*Pr$_2$), 1.11 (d, J=6.8 Hz, 3H, *p*-cymene-CH_3-*i*Pr), 0.94 ppm (d, J=6.8 Hz, 3H, *o*-aniline-CH_3-*i*Pr$_2$); ^{13}C NMR (101 MHz, $CDCl_3$): δ=187.60 (NHC carbon-Ru), 164.10, 143.87, 143.05, 140.23, 129.09, 125.80, 124.81, 123.61, 118.73, 110.81, 109.16, 90.41, 86.67, 85.85, 82.73, 46.92, 31.03, 27.85, 27.68, 25.74, 25.07, 23.85, 22.34, 19.07, 17.39, 15.31 ppm; ESI-MS (*m/z*): calcd for $C_{29}H_{41}ClN_3Ru$: 568.203; found: 568.008, [(η^6-*p*-cymene)Ru(L7)Cl]$^+$; elemental analysis calcd (%) for $C_{29}H_{41}N_3ClRuPF_6$: C 48.84, H 5.79, N 5.89; found: C 48.89, H 5.82, N 5.95.

[(η^6-*p*-Cymene)Ru(L8)Cl]PF$_6$ (8): Yield: 43.6 mg (60%). ^{1}H NMR (500 MHz, $CDCl_3$): δ=7.69 (s, 1H, imidazole-*H*), 7.44 (t, J=7.7 Hz, 1H, imidazole-*H*), 7.41–7.30 (m, 3H, Ar-*H*), 5.88 (d, J=5.8 Hz, 1H, *p*-cymene-*H*), 5.19 (d, J=6.0 Hz, 1H, *p*-cymene-*H*), 5.07 (d, J=6.0 Hz, 1H, *p*-cymene-*H*), 5.05 (d, J=5.9 Hz, 1H, *p*-cymene-*H*), 5.01–4.92 (m, 1H, N-C*H*-*i*Pr$_2$), 3.54–3.47 (m, 1H, *o*-aniline-C*H*-*i*Pr$_2$), 2.53–2.48 (m, 2H, *o*-aniline-C*H*-*i*Pr$_2$ and *p*-cymene-C*H*-*i*Pr$_2$), 2.43 (s, 3H, *p*-cymene-CH_3), 2.25 (s, 3H, imine-CH_3), 1.81 (d, J=6.6 Hz, 3H, N-CH_3-*i*Pr), 1.56 (d, J=6.4 Hz, 3H, *o*-aniline-CH_3-*i*Pr$_2$), 1.45 (d, J=6.5 Hz, 3H, N-CH_3-*i*Pr), 1.25 (d, J=6.6 Hz, 3H, *o*-aniline-CH_3-*i*Pr$_2$), 1.18 (d, J=6.6 Hz, 3H, *p*-cymene-CH_3-*i*Pr), 1.15 (d, J=6.4 Hz, 3H, *o*-aniline-CH_3-*i*Pr$_2$), 1.12 (d, J=6.8 Hz, 3H, *p*-cymene-CH_3-*i*Pr), 0.94 ppm (d, J=6.8 Hz, 3H, *o*-aniline-CH_3-*i*Pr$_2$); ^{13}C NMR (101 MHz, $CDCl_3$): δ=186.34 (NHC carbon-Ru), 164.09, 143.87, 143.09, 140.35, 129.09, 125.80, 124.82, 120.53, 119.31, 110.90, 109.14, 89.75, 86.92, 86.46, 82.10, 54.42, 30.91, 27.83, 27.67, 25.76, 25.09, 23.96, 23.84, 22.59, 22.50, 19.16, 17.42 ppm; ESI-MS (*m/z*): calcd for $C_{30}H_{43}ClN_3Ru$: 582.219; found: 582.42, [(η^6-*p*-cymene)Ru(L8)Cl]$^+$; elemental analysis calcd (%) for $C_{30}H_{43}N_3ClRuPF_6$: C 49.55, H 5.96, N 5.78; found: C 49.35, H 5.81, N 5.88.

[(η^6-*p*-Cymene)Ru(L9)Cl]PF$_6$ (9): Yield: 51.1 mg (69%). ^{1}H NMR (500 MHz, $CDCl_3$): δ=7.59 (d, J=2.1 Hz, 1H, imidazole-*H*), 7.43 (t, J=7.7 Hz, 1H, imidazole-*H*), 7.38–7.32 (m, 2H, Ar-*H*), 7.31 (d, J=2.1 Hz, 1H, Ar-*H*), 5.83 (d, J=6.2 Hz, 1H, *p*-cymene-*H*), 5.20 (d, J=6.0 Hz, 1H, *p*-cymene-*H*), 5.05 (d, J=6.1 Hz, 1H, *p*-cymene-*H*), 4.99 (d, J=6.2 Hz, 1H, *p*-cymene-*H*), 4.54–4.39 (m, 2H, *n*Bu-CH_2), 3.56–3.45 (m, 1H, *o*-aniline-C*H*-*i*Pr$_2$), 2.60–2.45 (m, 2H, *o*-aniline-C*H*-*i*Pr$_2$ and *p*-cymene-C*H*-*i*Pr$_2$), 2.42 (s, 3H, *p*-cymene-CH_3), 2.25 (s, 3H, imine-CH_3), 2.03–1.99 (m, 2H, *n*Bu-CH_2), 1.50–1.46 (m, 2H, *n*Bu-CH_2), 1.45 (d, J=6.7 Hz, 3H, *o*-aniline-CH_3-*i*Pr$_2$), 1.25 (d, J=6.6 Hz, 3H, *o*-aniline-CH_3-*i*Pr$_2$), 1.17 (d, J=7.0 Hz, 3H, *p*-cymene-CH_3-*i*Pr), 1.15 (d, J=6.6 Hz, 3H, *o*-aniline-CH_3-*i*Pr$_2$), 1.11 (d, J=6.8 Hz, 3H, *p*-cymene-CH_3-*i*Pr), 1.02 (t, J=7.3 Hz, 3H, *n*Bu-CH_3), 0.94 ppm (d, J=6.8 Hz, 3H, *o*-aniline-CH_3-*i*Pr$_2$); ^{13}C NMR (101 MHz, $CDCl_3$): δ=187.46 (NHC carbon-Ru), 164.14, 143.87, 143.04, 140.33, 129.10, 125.82, 124.83, 124.15, 118.53, 110.43, 109.51, 90.28, 86.77, 85.79, 82.66, 51.60, 31.61, 31.00, 27.85, 27.70, 25.80, 25.10, 25.04, 23.89, 23.80, 22.29, 19.95, 19.09, 17.37, 13.78 ppm; ESI-MS (*m/z*): calcd for $C_{31}H_{45}ClN_3Ru$: 596.235; found: 596.2108, [(η^6-*p*-cymene)Ru(L9)Cl]$^+$; elemental analysis calcd (%) for $C_{31}H_{45}N_3ClRuPF_6$: C 50.23, H 6.12, N 5.67; found: C 50.38, H 6.21, N 5.54. Crystals of complex **9** qualified for X-ray analysis were obtained by slow diffusion of petroleum ether into a concentrated solution of complex **9** in ethyl acetate.

[(η^6-*p*-Cymene)Ru(L10)Cl]PF$_6$ (10): Yield: 47.7 mg (65%). ^{1}H NMR (500 MHz, DMSO): δ=8.01 (d, J=2.4 Hz, 1H, imidazole-*H*), 7.59 (d, J=2.4 Hz, 2H, imidazole-*H* and Ar-*H*), 7.55 (t, J=7.4 Hz, 1H, Ar-*H*), 7.43 (s, 2H, Ar-*H*), 7.24 (d, J=7.4 Hz, 1H, Ar-*H*), 7.14 (t, J=7.6 Hz, 1H, Ar-*H*), 6.96 (d, J=7.5 Hz, 2H, Ar-*H*), 6.13 (d, J=6.3 Hz, 1H, *p*-cymene-*H*), 5.28 (d, J=6.0 Hz, 1H, *p*-cymene-*H*), 5.21 (d, J=6.3 Hz, 1H, *p*-cymene-*H*), 5.07–5.00 (m, 1H, N-C*H*-*i*Pr$_2$), 4.99 (d, J=5.9 Hz, 1H, *p*-cymene-*H*), 2.57 (s, 3H, *o*-aniline-CH_3), 2.55–2.51 (m, 1H, C*H*-*i*Pr$_2$), 2.21 (s, 3H, *p*-cymene-CH_3), 1.78 (s, 3H, *o*-aniline-CH_3), 1.73 (d, J=6.7 Hz, 3H, N-CH_3-*i*Pr), 1.46 (d, J=6.6 Hz, 3H, N-CH_3-*i*Pr), 1.16 (d, J=6.9 Hz, 3H, *p*-cymene-CH_3-*i*Pr), 1.14 ppm (d, J=6.9 Hz, 3H, *p*-cymene-CH_3-*i*Pr); ^{13}C NMR (101 MHz, DMSO): δ=192.68 (NHC carbon-Ru), 168.39, 153.04, 138.11, 137.97, 134.41, 134.23, 133.76, 133.66, 132.70, 131.14, 126.87, 126.07, 115.18, 113.74, 97.93, 91.75, 90.96, 89.80, 60.14, 58.91, 36.40, 28.71, 28.07, 27.65, 27.53, 25.40, 23.92, 23.46 ppm; ESI-MS (*m/z*): calcd for $C_{31}H_{37}ClN_3Ru$: 588.172; found: 588.007, [(η^6-*p*-cymene)Ru(L10)Cl]$^+$; elemental analysis calcd (%) for $C_{31}H_{37}N_3ClRuPF_6$: C 50.79, H 5.09, N 5.73; found: C 50.99, H 5.01, N 5.69.

Acknowledgments

We thank the National Natural Science Foundation of China (Grant No. 21671118) and the Taishan Scholars Program, Shandong Provincial Natural Science Foundation (ZR2018MB023), The Key Laboratory of Polymeric Composite & Functional Materials of Ministry of Education (PCFM-2017-01), Excellent Experiment project of Qufu Normal University (jp201705) for support.

Conflict of interest

The authors declare no conflict of interest.

Keywords: anticancer · imine-N-heterocyclic carbene · ruthenium(II) complexes · structure–activity relationship

[1] R. L. Siegel, K. D. Miller, A. Jemal, *CA-Cancer J. Clin.* **2018**, *68*, 7–30.
[2] a) L. H. Guo, W. J. Liu, C. L. Chen, *Mater. Chem. Front.* **2017**, *1*, 2487–2494; b) W. A. Herrmann, *Angew. Chem. Int. Ed.* **2002**, *41*, 1290–1309; *Angew. Chem.* **2002**, *114*, 1342–1363; c) L. H. Guo, S. Y. Dai, X. L. Sui, C. L. Chen, *ACS Catal.* **2016**, *6*, 428–441; d) L. H. Guo, C. L. Chen, *Sci. China Chem.* **2015**, *58*, 1663–1673.
[3] a) T. C. Johnstone, K. Suntharalingam, S. J. Lippard, *Chem. Rev.* **2016**, *116*, 3436–3486; b) Z. Liu, P. J. Sadler, *Acc. Chem. Res.* **2014**, *47*, 1174–1185; c) G. Shi, S. Monro, R. Hennigar, J. Colpitts, J. Fong, K. Kasimova, H. Yin, R. DeCoste, C. Spencer, L. Chamberlain, A. Mandel, L. Lilgec, S. A. McFarland, *Coord. Chem. Rev.* **2015**, *282–283*, 127–138; d) F. Li, J. G. Collins, F. R. Keene, *Chem. Soc. Rev.* **2015**, *44*, 2529–2542; e) K. B. Garbutcheon-Singh, M. P. Grant, B. W. Harper, A. M. Krause-Heuer, M. Manohar, N.

Orkey, J. R. Aldrich-Wright, *Curr. Top. Med. Chem.* **2011**, *11*, 521 – 542; f) N. Muhammad, Z. J. Guo, *Curr. Opin. Chem. Biol.* **2014**, *19*, 144 – 153.
[4] a) V. Cepeda, M. A. Fuertes, J. Castilla, C. Alonso, C. Quevedo, J. M. Pérez, *Anti-Cancer Agents Med. Chem.* **2007**, *7*, 3 – 18; b) E. R. Jamieson, S. J. Lippard, *Chem. Rev.* **1999**, *99*, 2467 – 2498; c) G. Chu, *J. Biol. Chem.* **1994**, *269*, 787 – 790.
[5] a) L. Kelland, *Nat. Rev. Cancer* **2007**, *7*, 573 – 584; b) L. Galluzzi, L. Senovilla, I. Vitale, J. Michels, I. Martins, O. Kepp, M. Castedo, G. Kroemer, *Oncogene* **2012**, *31*, 1869 – 1883; c) Y. Y. You, H. Hu, L. Z. He, T. F. Chen, *Chem. Asian J.* **2015**, *10*, 2744 – 2754.
[6] a) A. Leonidova, G. Gasser, *ACS Chem. Biol.* **2014**, *9*, 2180 – 2193; b) Y. L. Yang, L. H. Guo, Z. Z. Tian, Y. T. Gong, H. M. Zheng, S. M. Zhang, Z. S. Xu, X. X. Ge, Z. Liu, *Inorg. Chem.* **2018**, DOI: 10.1021/acs.inorgchem.8b01656. c) Q. Du, L. H. Guo, M. Tian, X. X. Ge, Y. L. Yang, X. Y. Jian, Z. S. Xu, Z. Z. Tian, Z. Liu, *Organometallics* **2018**, DOI: 10.1021/acs.organomet.8b00402.
[7] a) C. G. Hartinger, N. Metzler-Nolte, P. J. Dyson, *Organometallics* **2012**, *31*, 5677 – 5685; b) M. R. Gill, J. A. Thomas, *Chem. Soc. Rev.* **2012**, *41*, 3179 – 3192; c) M. Li, L. H. Lai, Z. N. Zhao, T. F. Chen, *Chem. Asian J.* **2016**, *11*, 310 – 320; d) N. P. Barry, P. J. Sadler, *Chem. Commun.* **2013**, *49*, 5106 – 5131; e) K. Suntharalingam, W. Lin, T. C. Johnstone, P. M. Bruno, Y. R. Zheng, M. T. Hemann, S. J. Lippard, *J. Am. Chem. Soc.* **2014**, *136*, 14413 – 14416; f) C. Scolaro, A. Bergamo, L. Brescacin, R. Delfino, M. Cocchietto, G. Laurenczy, T. J. Geldbach, G. Sava, P. J. Dyson, *J. Med. Chem.* **2005**, *48*, 4161 – 4171; g) C. H. Leung, H. J. Zhong, D. S. H. Chan, D. L. Ma, *Coord. Chem. Rev.* **2013**, *257*, 1764 – 1776; h) B. Y. W. Man, H. M. Chan, C. H. Leung, D. S. H. Chan, L. P. Bai, Z. H. Jiang, H. W. Li, D. L. Ma, *Chem. Sci.* **2011**, *2*, 917 – 921.
[8] a) L. Biancalana, L. K. Batchelor, T. Funaioli, S. Zacchini, M. Bortoluzzi, G. Pampaloni, P. J. Dyson, F. Marchetti, *Inorg. Chem.* **2018**, *57*, 6669 – 6685; b) M. Tian, J. J. Li, S. M. Zhang, L. H. Guo, X. D. He, D. L. Kong, H. R. Zhang, Z. Liu, *Chem. Commun.* **2017**, *53*, 12810 – 12813; c) J. J. Li, L. H. Guo, Z. Z. Tian, M. Tian, S. M. Zhang, K. Xu, Y. C. Qian, Z. Liu, *Dalton Trans.* **2017**, *46*, 15520 – 15534; d) S. Movassaghi, S. Singh, A. Mansur, K. K. H. Tong, M. Hanif, H. U. Holtkamp, T. Söhnel, S. M. F. Jamieson, C. G. Hartinger, *Organometallics* **2018**, *37*, 1575 – 1584.
[9] L. Oehninger, M. Stefanopoulou, H. Alborzinia, J. Schur, S. Ludewig, K. Namikawa, A. Muñoz-Castro, R. W. Köster, K. Baumann, S. Wölfl, *Dalton Trans.* **2013**, *42*, 1657 – 1666.
[10] L. Biancalana, S. Zacchini, N. Ferri, M. G. Lupo, G. Pampaloni, F. Marchetti, *Dalton Trans.* **2017**, *46*, 16589 – 16604.
[11] Y. Li, B. Liu, X. R. Lu, M. F. Li, L. N. Ji, Z. W. Mao, *Dalton Trans.* **2017**, *46*, 11363 – 11371.
[12] Z. Liu, A. Habtemariam, A. M. Pizarro, S. A. Fletcher, A. Kisova, O. Vrana, L. Salassa, P. C. A. Bruijnincx, G. J. Clarkson, V. Brabec, P. J. Sadler, *J. Med. Chem.* **2011**, *54*, 3011 – 3026.
[13] S. Karmakar, S. Chatterjee, K. Purkait, A. Mukherjee, *Dalton Trans.* **2016**, *45*, 11710 – 11722.
[14] a) Z. Liu, R. J. Deeth, J. S. Butler, A. Habtemariam, M. E. Newton, P. J. Sadler, *Angew. Chem. Int. Ed.* **2013**, *52*, 4194 – 4197; *Angew. Chem.* **2013**, *125*, 4288 – 4291; b) H. R. Zhang, L. H. Guo, Z. Z. Tian, M. Tian, S. M. Zhang, Z. S. Xu, P. W. Gong, X. F. Zheng, J. Zhao, Z. Liu, *Chem. Commun.* **2018**, *54*, 4421 – 4424.
[15] H. Y. Huang, P. Y. Zhang, B. L. Yu, Y. Chen, J. Q. Wang, L. N. Ji, H. Chao, *J. Med. Chem.* **2014**, *57*, 8971 – 8983.
[16] a) V. Novohradsky, J. Yellol, O. Stuchlikova, M. D. Santana, H. Kostrhunova, G. Yellol, J. Kasparkova, D. Bautista, J. Ruiz, V. Brabec, *Chem. Eur. J.* **2017**, *23*, 15294 – 15299; b) M. H. Chen, F. X. Wang, J. J. Cao, C. P. Tan, L. N. Ji, Z. W. Mao, *ACS Appl. Mater. Interfaces* **2017**, *9*, 13304 – 13314.
[17] H. Wang, J. A. Joseph, *Free Radical Biol. Med.* **1999**, *27*, 612 – 616.
[18] a) P. Saftig, J. Klumperman, *Nat. Rev. Mol. Cell Biol.* **2009**, *10*, 623 – 635; b) M. E. Guicciardi, M. Leist, G. J. Gores, *Oncogene* **2004**, *23*, 2881 – 2890; c) G. Kroemer, M. Jäättelä, *Nat. Rev. Cancer* **2005**, *5*, 886 – 897; d) H. C. Chen, J. W. Tian, W. J. He, Z. J. Guo, *J. Am. Chem. Soc.* **2015**, *137*, 1539 – 1547.
[19] P. Boya, G. Kroemer, *Oncogene* **2008**, *27*, 6434 – 6451.
[20] S. B. Jensen, S. J. Rodger, M. D. Spicer, *J. Organomet. Chem.* **1998**, *556*, 151 – 158.
[21] a) J. A. Deng, H. Y. Gao, F. M. Zhu, Q. Wu, *Organometallics* **2013**, *32*, 4507 – 4515; b) M. L. Rosenberg, E. Langseth, A. Krivokapic, N. S. Gupta, M. Tilset, *New J. Chem.* **2011**, *35*, 2306 – 2313; c) M. Frøseth, K. A. Netland, C. Rømming, M. Tilset, *J. Organomet. Chem.* **2005**, *690*, 6125 – 6132; d) M. L. Rosenberg, A. Krivokapic, M. Tilset, *Org. Lett.* **2009**, *11*, 547 – 550; e) S. Dastgir, K. S. Coleman, A. R. Cowley, M. L. H. Green, *Organometallics* **2006**, *25*, 300 – 306; f) A. Krajete, G. Steiner, H. Kopacka, K. H. Ongania, K. Wurst, M. O. Kristen, P. Preishuber-Pflügl, B. Bildstein, *Eur. J. Inorg. Chem.* **2004**, 1740 – 1752.

Manuscript received: July 7, 2018
Revised manuscript received: August 3, 2018
Accepted manuscript online: August 12, 2018
Version of record online: ■■ ▮▮, 0000

FULL PAPER

Anticancer Complexes

Yuliang Yang, Lihua Guo, Zhenzhen Tian, Xicheng Liu, Yuteng Gong, Hongmei Zheng, Xingxing Ge, Zhe Liu**

■■ – ■■

Imine-N-Heterocyclic Carbenes as Versatile Ligands in Ruthenium(II) *p*-Cymene Anticancer Complexes: A Structure–Activity Relationship Study

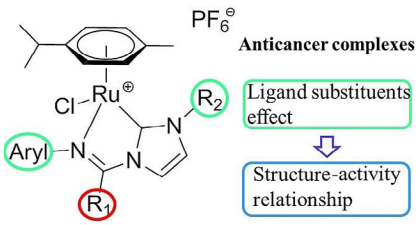

Ruthenium anticancer complexes: A series of novel ruthenium(II) *p*-cymene complexes bearing versatile imine-N-heterocyclic carbene ligands were synthesized and characterized. The cytotoxicity of these complexes showed significant structure–activity relationships. In addition, the mechanism of actions (MoAs) of these complexes was explored by flow cytometry and confocal microscopy imaging.